Calibration of the SOAR speckle data: the 5th iteration

Authors:*A. Tokovinin*
Version: 3
Date: 2025-11-12
File: prj/speckle/doc/SAM24/recalib/calibration.tex

Abstract: Calibration of speckle interferometry at SOAR is based on the observations of relatively wide pairs with well-modeled motion. These models are updated here using data till 2025.77, and the overall accuracy of the astrometric calibration is estimated as 0.16% in pixel scale and 0.09° in angle. Such accuracy is still insufficient compared to the typical internal measurement errors of 0.3 mas, so the typical position errors of 1″ pairs, 1.6 mas, are dominated by the calibration uncertainty. There are no systematic differences of relative astrometry between SOAR and Gaia. Frequent and accurate measurements revealed wobble caused by inner subsystems in two binaries used previously for calibration.

1 Introduction

Speckle interferometry has replaced the traditional visual techniques of double-star measurement in the end of the 20th century. When used at large telescopes with linear detectors and suitable data processing, it reaches a very high astrometric precision. For example, the median internal error of 1922 position measurements at the 4.1 m SOAR telescope reported in (Tokovinin et al., 2024) is 0.3 mas in both radial (in separation) and tangential directions. However, reaching a comparable *accuracy* is challenging because calibration of the orientation and pixel scale is often the dominant errors source. For a 1″ pair, the median internal error corresponds to a relative scale error of 3 10^{-4} (0.03%) or an angle error of 0.017°. The accuracy of current calibration is substantially less, and the calibration errors dominate, except at small separations.

Most orbits of visual binaries are based on the historic micrometer measurements of much inferior accuracy than speckle. Even if only reliable orbits are used for calibration of scale and orientation, as done by some speckle programs, the astrometric potential of speckle interferometry is lost. This fact was realized by McAlister (1977) who implemented an independent and more accurate calibration strategy. They placed a double-slit mask in front of the 4 m telescope, measured the period and orientation of the fringes from single stars observed with this mask, and, knowing the wavelength of the narow-band filter, determined the calibration parameters. This absolute calibration was "transferred" to smaller telescopes via observations of common relatively wide pairs.

A program of high-precision astrometry of visual binaries in search of inner planetray companions was undertaken by Muterspaugh et al. using the Mark III long-baseline interferometer (Muterspaugh et al., 2010). This astrometry is much more accurate and precise than speckle. However, binary stars change their positions, and the orbits based partially on the Mark III data become less accurate with time. Very accurate relative positions of a few binaries measured occasionally by other interferometers (NPOI, VLTI) can be used for calibration if their motion is well modeled.

Space astrometric missions, Hipparcos and Gaia, provided accurate relative positions of many binaries. However, the small 0.3 m aperture of Hipparcos did not allow it to reach a very high precision:

the relative positions have errors on the order of 10 mas, must larger than speckle interferometry at 4 m telescopes. Gaia with its 1 m apertures has a better potential. It resolves pairs wider than $\sim 0.8''$ as two sources, allowing calculation of their relative positions. Although Gaia astrometry of single bright stars is extremely accurate, proximity of the components creates certain problems for double stars (see below).

Here I describe the absolute calibration of speckle-interferometric measurements of double stars performed with the high-resolution camera (HRCam) at the 4.1 m SOAR telescope. This includes one observing run at the Blanco telescope in 2008.5. HRCam was used for the first time at SOAR in 2007.7 on an engineering night. Several relatively wide pairs were observed for calibration. At that time, their positions were poorly known, so the published measures from this first HRCam run had large systematic errors. However, the relative motion of those pairs was subsequently well-modeled, allowing posterior correction. This principle is the cornerstone of the HRCam calibration strategy. Several relatively wide pairs with slow motion, *calibrators*, are observed in each run together with the main program. Although the orbits of "slow" pairs are usually of low quality or do not exist, the small observed arcs can be accurately modeled, allowing calibration of the pixel scale and orientation. As the calibrator models improve with time, the accuracy of the old (published) data can be improved as well by retroactive calibration.

In 2009, an effort to calibrate the HRCam on the absolute scale has been untertaken. An interferometer with a 0.5 m baseline projected narrow beams from a green laser pointer into the telescope, and the period and orientation of the resulting fringes at the focal plane delivered the calibration parameters (Tokovinin et al., 2010, Sect. 2.5). This method, similar to the slit mask, has its limitations in accuracy and requires physical intervention at the telescope. In the folowing HRCam runs, the pixel scale and orientation were controlled internally by taking images of a point source at the telescope focal plane that was translated under remote control (this source is part of the SOAR Adaptive Module, it is permanently available). The scale at the focal plane, assumed to be known from the telescope optical prescription, was thus related to the HRCam pixels. Measurements revealed this relation to be very stable in time. Orientation on the sky was checked by taking sky images in a wider field using the SAM imager and relating the resulting angle offset to the same internal point-source reference in the focal plane.

The science use of the HRCam has increased sharply in 2014, calling for a simpler and more accurate calibraion of each observing run. The first set of 41 calibrator binaries was identified in 2014 by selecting pairs with a large number of HRCam observations and a good time coverage in 2008-2014. This selection was opportunistic in the sense that the calibrators were not chosen in advance but rather picked up from the available observational material. The set of calibrators was revised in the subsequent iterations. Frequently observed triple stars (resolved binaries with inner subsystems) were excluded. The separations and angles were approximated by linear functions of time and used to calibrate the ongoing runs. As more data became available, the set of calibrators was revised, and their modeling was repeated. Table 1 lists five iterations of this process; the last one, CAL5, is described here.

SOAR has an alt-azimuth mount and a rotator at the Nasmith port which maintains the chosen position angle on the sky as the telescope tracks. The angle of the rotator is computed by the telescope control system using the current telescope pointing model which accounts for small deviations from a perfectly aligned mount. Errors of the pointing model translate into errors of the rotator angle, being strongest near the zenith. Furthermore, the tape encoder of the SOAR Nasmith rotator had a problem

Table 1: Calibration of HRCam on wide binaries

Iteration	Date last	N	Reference
CAL1	2014.76	41	Tokovinin et al. (2015)
CAL2	2017.53	64	Tokovinin et al. (2018)
CAL3	2019.7	62	Tokovinin et al. (2020)
CAL4	2021.75	112	Tokovinin et al. (2022)
CAL5	2025.77	86	This work

of the missing counts, in particular when it passed through zero (this was fixed in 2020). So, there is always an offset between the desired and real position angle on the sky that depends on time (owing to the missing encoder counts) and orientation (owing to the pointing model errors). As to the pixel scale, the image on the HRCam detector is formed after reflection from the SAM deformable mirror. If its curvature changes affect the focus distance, compensated by focusing the telescope, hence pixel scale is affected. These considerations imply that there are limits on the calibration accuracy imposed by the telescope and instrument. I do not know whether these limits have been reached or not.

2 Calibrator models

As stated above, the slow motion of a wide binary can be represented by linear functions of time in polar coordinates (ρ, θ):

$$\theta(t) = \theta_0 + \theta_1(t - t_0), \quad (1)$$

$$\rho(t) = \rho_0 + \rho_1(t - t_0), \quad (2)$$

where t_0 is the mean time of observation. These equations describe a spiral trajectory. Fragment of a spiral is a better match to an orbital segment than a linear trajectory in rectangular coordinates, with the same number of 5 free parameters (for a circular face-on orbit, the spiral is accurate). The choice of t_0 ensures that the offsets and slopes are statistically independent.

Many calibrators are nearby pairs with detectable orbital motion (some with know orbits). They were frequently observed for monitoring their motion and became calibrators for this reason. Naturally, such pairs measurably deviate from the linear models. Their observed arcs are much better described by 7 elements of Keplerian orbits. However, considering the uncertain nature of long-period orbits and their reliance on the old inaccurate data, the orbits need adjustment to match the SOAR data. The orbits of calibrators tuned to model our data are not necessarily better than their published versions. In some cases, a full revision of the orbits was necessary to reach satisfactory representation of the observed arcs. The orbital models were used starting from CAL2.

Initially, only three elements of the published orbits, t_0, a, and Ω , were fitted to the arcs covered by the SOAR data, leaving other elements fixed. However, this proved to be insufficient when the catalog orbits were inaccurate (especially at short periods) or obviously incorrect, as revealed by the inconsistent mass sums derived from these orbits and parallaxes. Several incorrect orbits of our calibrators published by Izmailov (2019) were poorly constrained by the short observed arcs and inaccurate visual measurements. In such cases, I revised the orbits and fitted the 3 elements to those revisions. These revisions have reduced the residuals of the SOAR data significantly.

The `orbit` code used to fit the elements corrects the position angles for precession internally, so the node Ω refers to the J2000.0 epoch, while the measured angles $\theta(t)$ refer to the equinox at time t. The ephemeris computed from the orbital elements gives angles for the J2000.0 equinox, and a precession in angle is added to translate them to the time t for comparison with the measurements. The precession is linear in time, it is absorbed in the slope θ_1, so for the linear models the precession correction is not needed.

The process of fitting the models is iterative. With the initial orbital and linear models, systematic errors of each observing run are determined and saved. The data are corrected for these errors at the next iteration, leading to better models, etc. In the end, a consistent set of models and run corrections is obtained. After correcting for the run systematics, the measurements are on the same "system".

Calibration on binaries cannot reveal common errors of the scale and orientation, so an external reference is needed. Such a reference is now available from the Gaia data release 3 (DR3). It gives positions for $t = 2016.0$ and equinox J2000.0, and the calibrator models can be reliably interpolated to this date for comparison. The 4th iteration CAL4 revealed a systematic difference with Gaia (Tokovinin et al., 2022): an offset of $-0.21°$ in angle and the pixel scale 1.0053 times larger than needed. The models were corrected for this effect, and starting from 2021.0 the internally calibrated measures are no longer biased (see below). The measurements before 2021.0 used here are corrected, so they differ slightly from the published values. The calibration errors of the past observing runs determined by CAL4 are also removed. So, the data used for the CAL5 iteration are free from the systematics and reasonably well corrected for the past calibration errors, although the run-dependent offsets are still measurable (see below).

3 The 5th revised calibration

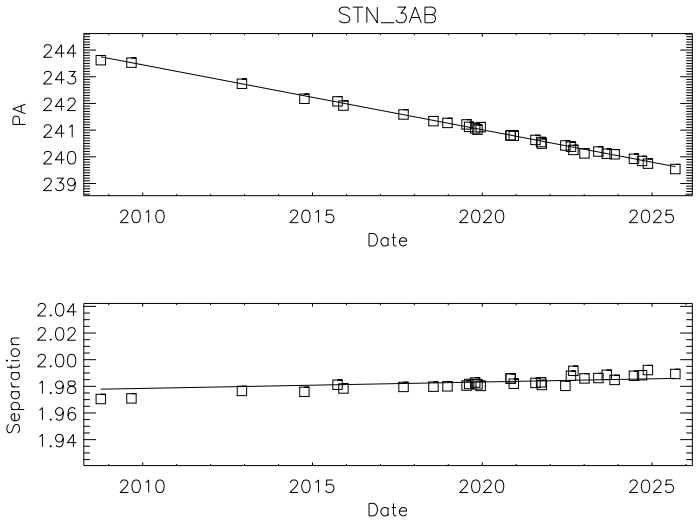

Figure 1: Data on the calibrator STN 3AB (00522-2237) with linear model (lines) and observations (squares). The rms residuals are 2.0/3.5 mas in the tangential and radial directions, respectively.

I started with a list of 104 calibrators used in CAL4. The code `recalib5.pro`, almost identical to `recalib4.pro`, ingests the list into a structure `recalib` which contains the WDS code, name, HIP number, mean separation, magnitude difference, and type of the model (1 — linear, 2 — orbit). The SOAR observations of each pair are collected and complemented by the Hipparcos position, if available, to extend the time line.

The calibrators are examined individually by plotting the position angles and separations and their models using `plotstar`, as illustrated in Fig. 1 (the HIP measures are not considered). The rms residuals σ to the model in the tangential and radial directions (hereafter tan/rad) are printed. The code identifies outliers that exceed 2.5σ; they can be removed from the data ("killed"), and the model can be refined. A pair can be excluded from CAL5. Two cases of triple stars that show obvious wobble are identified and removed (they are discussed below). I removed calibrators with magnitude difference exceeding 3 mag, fainter than 9th mag, closer than $0.5''$, or with few observations. The final CAL5 set contains 86 pairs: 13 with linear models and 73 with orbits. In one case (WDS 07448−3344, STN9001), the orbit was computed because deviations from the linear model were large and systematic, so the model type was changed from 1 (linear) to 2 (orbital).

The orbits are fitted using `orbit.pro`. The initial input files `*.inp` are produced automatically for all orbital pairs, with the elements taken from ORB6 (its private, updated version in IDL format is used). They contain only SOAR and HIP measures with assigned errors of 2 and 10 mas, respectively. By default, only three elements T, a, Ω are fitted to the SOAR positions, leaving all other elements at their initial values. This is based on the assumption that the orbit gives a good representation of the observed arc, and the adjustment of angle, scale, and time is sufficient to match the SOAR data. In a number of cases, this assumption was obviously incorrect, the observed arc deviated from the orbit in a systematic way after the adjustment. Some catalog orbits have inconsistent mass sums derived from the elements and parallaxes. Several incorrect orbits of our calibrators published by Izmailov (2019) were poorly constrained by the short observed arcs and inaccurate visual measurements. In such cases, I revised the orbits and fitted the 3 elements to those revisions. These revisions have reduced the residuals of the SOAR data significantly. For WDS 17190−3459 (MLO 4AB) with a period of 42 yr, a substantial arc is covered at SOAR, allowing a full orbit fit based only on the SOAR data.

The CAL5 set was scrutinized with particular attention to residuals exceeding 5 mas. Killing of 1-2 outliers and/or orbit adjustment helped to diminish the residuals to an average level of 1-3 mas.

4 Properties of CAL5

Figure 2 characterizes the rms residuals of the CAL5 set. On the left, the cumulative distributions are shown. The tan and rad residuals are very similar, their medians are 1.78 and 1.72 mas, respectively. The right-side plot shows that residuals increase with angular separation ρ. The tan and rad residuals behave in a similar way. The common linear fit is

$$\sigma \approx 0.65 + 1.10\rho \ \ [\text{mas}]. \tag{3}$$

Alternatively, a line passing through coordinate origin describes the residuals quite well. The median slopes in tangential and radial directions are again similar (1.63 and 1.65 mas/arcsec), and the mean slope of 1.64 is shown in Fig. 2.

A linear dependence on ρ suggests that the residuals are dominated by imperfect models. The error of 1.6 mas at $1''$ separation corresponds to the relative uncertainty of the pixel scale of 0.0016 or

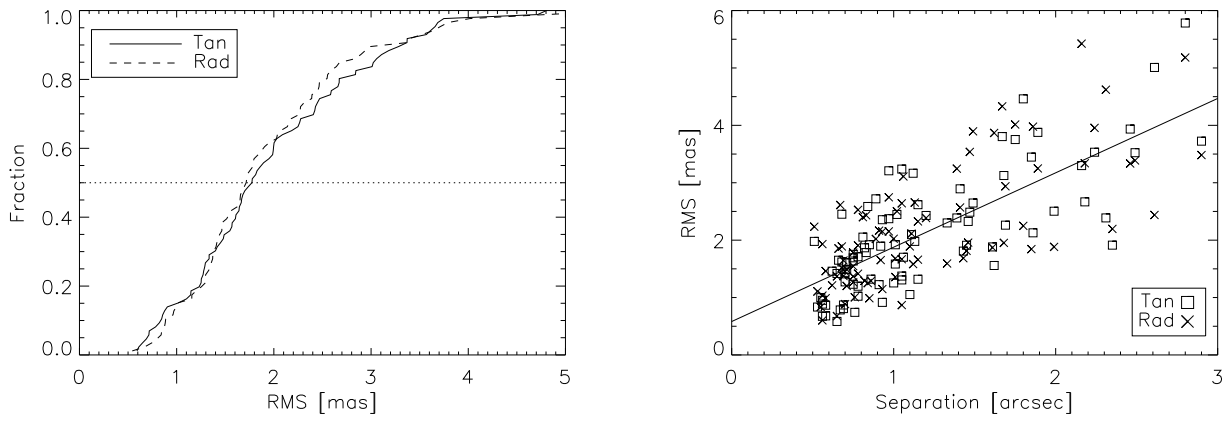

Figure 2: **Left:** cumulative histogram of the tan/rad rms residuals. **Right:** dependence of the residuals on the separation; the line has a slope of 1.64 mas/arcsec.

0.16%, or to an angle error of 0.09°. Compare this plot with CAL4 (Fig. 1 in Tokovinin et al. (2022)), where the linear fit was similar, but there were more outliers with large rms.

Note a group of points in Fig. 2, right, at $\rho \sim 0.6''$ with larger residuals. They correspond to pairs with fast motion where a future orbit improvement could help. If the residuals were dominated by the turbulence-induced differential image motion, they would increase with ρ faster in the rad direction than in tan, but this is not the case here. The turbulence error should be about 0.5 mas at $1''$ separation, as estimated by Tokovinin et al. (2022).

With the revised CAL5 models, individual runs can be re-calibrated retroactively using `fitruns`. Figure 3 shows the result for the 132 observing runs with HRCam. Only 3 runs do not have any calibrator observations. The median and mean number of calibrator observations in each run is 11 and 13.7, respectively. The median absolute correction in angle is 0.053°, its median rms scatter in individual runs is 0.082°. The median absolute deviation of the relative scale from one is 0.00090 (0.09%), its median rms scatter is 0.0015. These results indicate that the observations are already well corrected for the run-to-run calibration errors at the level compatible to the overall accuracy of CAL 5 models, 0.15%. Note the reduced scatter after 2017, when a new EM CCD was installed in HRCam and the calibrators were observed systematically in sufficient number.

Four observing runs (in 2014.76, 2014.85, and two in 2016.95) used a replacement camera Luca-R with poor vertical charge transfer causing a loss of resolution along columns for fainter stars. These data of lower quality were deleted for some calibrators; an increased scatter can be noted in Figure 3 for these dates.

The set of CAL5 models is consistent not only internally, but also externally. Relative positions reported in the Gaia DR3, computed from the coordinates of the two sources, are available for 54 pairs. The Gaia positions are compared to the CAL5 positions for 2016.0 in Fig. 4. Discrepant Gaia positions are ignored. For the 51 pairs where the Gaia and CAL5 separations differ by less than 20 mas, the rms difference is 2.8 mas. The mean scale difference is 1.2E-5, and the rms scatter of the scale deduced for each pair individually is 0.0012 (similar to the internal quality of the CAL5 models estimated above). The number of Gaia position angles that differ from CAL5 by more than

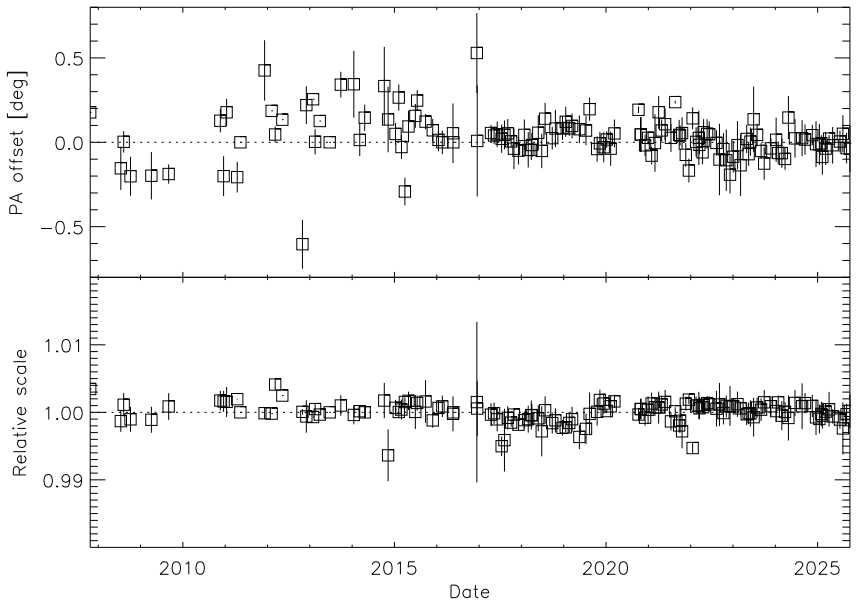

Figure 3: Calibration parameters of 132 individual observing runs. The error bars correspond to the $\pm\sigma$ scatter between calibrators in each run. These corrections are applied to the archival SOAR data.

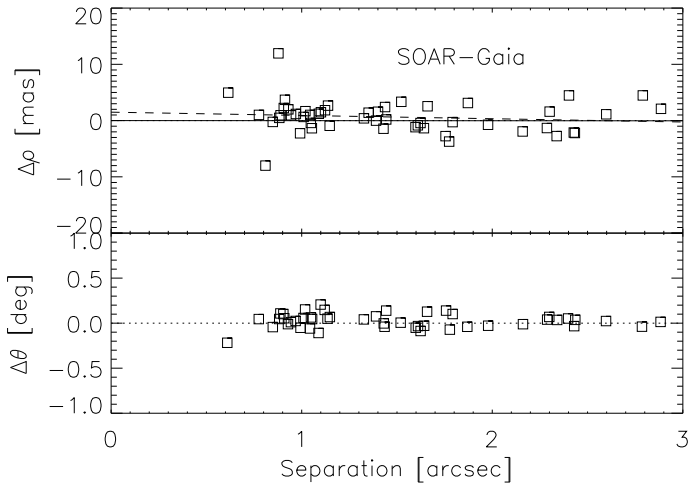

Figure 4: Comparison of CAL5 with Gaia DR3. Dashed line in the upper plot is a formal linear fit.

1° is 6, larger than the outliers in separation. For the remaining "good" 48 pairs, the mean difference in position angle SOAR−Gaia is +0.022°, the scatter is 0.036°, and the rms in the tan direction is 1.77 mas.

All pairs with discrepant Gaia positions have problematic astrometry where one or both components do not have 5-parameter solutions in DR3. Problems of Gaia astrometry of such binaries are detailed by Holl et al. (2023). One of the major factors seems to be the mixture of resolved and unresolved scans, expected to affect mostly the position angle. The largest discrepancy in angle, $-23°$, is found for WDS 15351−4110 ($\rho = 0.83''$) where both components lack 5-parameter DR3 solutions. Another pair discrepant by 10° is WDS J19064−3704 ($\rho = 1.47''$), where components with similar fluxes could be swapped in some Gaia scans.

5 Astrometric error budget

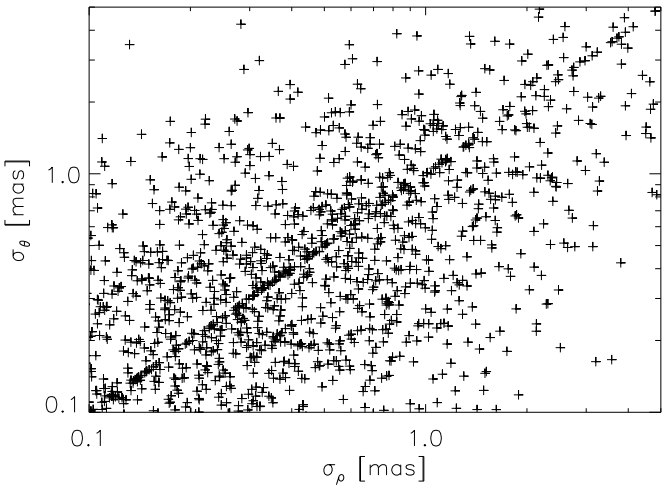

Figure 5: Comparison between radial σ_ρ and tangential σ_θ position errors in the SOAR data of 2023.

Contribution of the calibration errors to the overall error budget of speckle astrometry at SOAR is explored using measurements of resolved binaries made in 2023 (Tokovinin et al., 2024). The internal error σ_i assigned by the pipeline is the largest of the error σ_1 determined by fitting the binary-star model to the speckle power spectrum (average error in X and Y) and the rms scatter σ_2 between measurements deduced from several data cubes. In most cases, two measurements per target are available, so $\sigma_2 = \sqrt{2}\Delta$, where Δ is the absolute difference between two measures. The internal errors in the rad and tan directions are computed independently and published in the table of measures. Statistically, the rad and tan errors are similar. Their medians are 0.30 mas, and they are slightly correlated, as shown in Fig. 5. Points on the diagonal correspond to the cases where $\sigma_1 > \sigma_2$, so both errors equal σ_1. Here data with $\sigma_i > 5$ mas (mostly for very faint targets) are ignored, and the remaining 1871 estimates (out of 1913 total) are considered.

Adopting a conservative approach, let us assume that the internal measurement error is a maximum of σ_i in both directions; its median is 0.44 mas. Adding quadratically the estimated calibration error $C\rho$, where $c = 0.0016$ is the relative uncertainty estimated above, the external error σ_e can be estimated

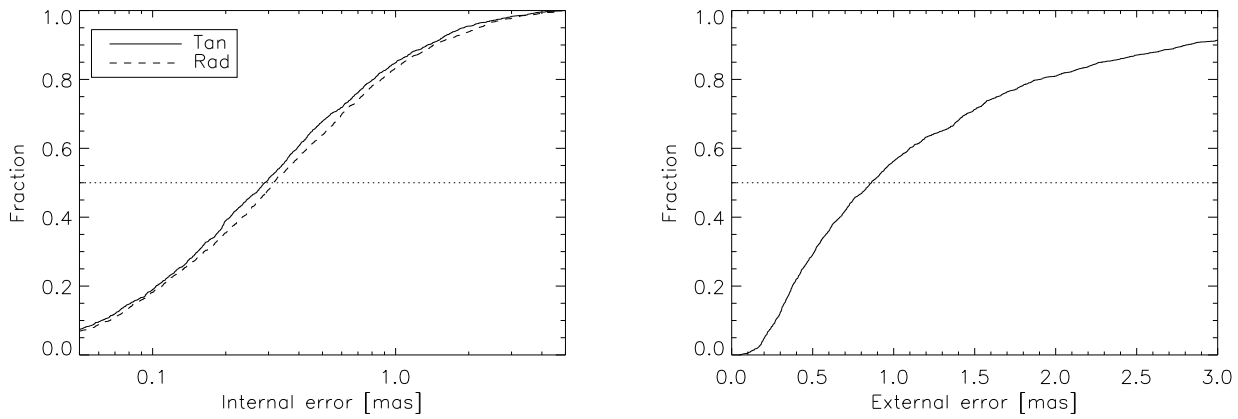

Figure 6: Cumulative distributions of internal errors (left, log scale) and of the estimated external errors (right, linear scale).

as their quadratic sum:

$$\sigma_e^2 = \sigma_i^2 + (C\rho)^2. \tag{4}$$

Cumulative distributions of internal and external errors are shown in Fig. 6. The median external error is 0.86 mas. The median separation of $0.16''$, which corresponds to the calibration error $C\rho$ of 0.26 mas, so for most close pairs the calibration errors are a minor contributor.

The above estimate of the internal errors is conservative. Averaging ∼10 calibrator observations per run could reduce the scale and angle errors up to a factor of 3 (if the errors are normally distributed, which is not the case). The reduction of internal errors owing to averaging of two measures per target is also neglected here. On the other hand, the internal errors could be larger than published owing to a contribution from imperfect models of speckle power spectra caused by instrumental effects (aberrations, vibrations). Their influence is reduced, albeit partially, when reference point sources are observed, but references are not available for all targets.

6 Triple stars

Improved accuracy of the HRCam calibration and frequent measures of the calibrators reveal cases where their motion deviates from the models in a systematic way. These pairs experience "wobble" caused by inner subsystems, they are hierarchical triple stars. One such wobbling ex-calibrator, BU 83, is presented in (Tokovinin et al., 2018). The two newly discovered triple calibrators, WDS 01316−5322 (I 264AB) and 18250−0135 (AC 11) are discussed in (Tokovinin, 2025). Their discovery is a direct consequence of the accurate and consistent calibration.

Quite likely, some of the remaining calibrators contain unknown inner subsystems causing a tiny wobble and increasing the residuals. Two wobble candidates with larger-than-normal residuals are WDS 06048−4828 (DUN 23, 4.9/6.6 mas) and 16309+0159 (STF 2055AB, 3.4/1.7 mas). The residuals do not decrease after removing a few outliers. However, they do not show any obvious periodic behaviour. In the first pair, Gaia DR3 determined parallaxes of both components, with an increased

RUWE=2.0 for the primary. In STF 2955, Gaia gives no astrometric solutions for both stars, despite their separation of 1.39″, while the relative position in Gaia agrees with the SOAR model for this pair.

7 Discussion: pros and cons

The calibration strategy based on wide pairs is practical and attractive. One of its strengths is the ability to check and correct existing measures. However, there are weaknesses as well. The most obvious problem is that the models of calibrators degrade with time and need regular updates. The second caveat is that the models are never perfect and might be a significant contributor to the calibration errors. Finally, with accurate data some calibrators are revealed as triple stars with wobble. An obvious sortcoming of the current SOAR calibrators is their ad hoc nature: these pairs were selected based on the data availability, not because they were the best choice. Some calibrators became too close (below 0.5″) or too wide (above 3.2″) and are no longer observed for this reason.

A potential improvement might consist in selecting a new set of calibrators from scratch. It could be based on known bright pairs with slow motion (i.e. distant) and good Gaia astrometry (small RUWE). The Gaia DR3 already provides linear models of such pairs that predict accurate relative positions for 2016.0 and degrade with time mildly owing to PM errors. Future Gaia data releases will improve these models, and they will eventually cover the full period of Gaia operation, 2014-2025.

Yet another calibration strategy, adopted by some AO instruments, consists in observations of astrometric standards, e.g. the Orion trapezium with NACO at VLT or the globular clusters with Keck AO. The AO systems typically have wider field of view compared to the speckle cameras, facilitating good astrometry. A speckle instrument with a variable plate scale can be calibrated in this way: an astrometric solution for an image in wide field can be used to calibrate the narrow field, if the relation between these two modes is established by an internal calibration (e.g. using a pinhole mask or laser fringes).

References

Holl, B., Fabricius, C., Portell, J., et al. 2023, A&A, 674, A25

McAlister, H. A. 1977, ApJ, 215, 159

Muterspaugh, M. W., Lane, B. F., Kulkarni, S. R. et al. 2010, AJ, 140, 1579

Tokovinin A., Mason B.D., Hartkopf W.I. 2010, AJ, 139, 743

Tokovinin, A., Mason, B.D., Hartkopf, W.I., Mendez, R.A., Horch, E.P. 2015, AJ, 150, 50

Tokovinin, A., A., Mason, B.D., Hartkopf, W.I., Mendez, R.A., Horch, E.P. 2018, AJ, 155, 235

Tokovinin, A., Mason, B. D., Mendez, R. A., Costa, E., Horch, E. P. 2020, AJ, 160, 7

Tokovinin, A., Mason, B.D., Mendez, R.A., Costa, E. 2022, AJ, 164, 58

Tokovinin, A., Mason, B. D., Mendez, R. A., Costa, E. 2024, AJ, 168, 28

Tokovinin, A., Orbits of Twelve Multiple Stars. Submitted to AJ 2025-11-01